Other	ALOX5AP, CD9, FLI1, GUSB, HPGD, IL13RA1, INPP5D, ISG15, LCN2, **LGAL53**, LXN, MET, OSMR, P2RX7, S100A4, SOX9, SRGN, SYNPO, TF

[a]Genes in the SCC are indicated in bold

A potential sequence of reactive changes has been proposed by Hwang *et al.* and we have been able to identify genes in our SCC and core network at each stage in this proposed sequence. Transcriptome analysis suggested that one of the first changes was the activation of the complement pathways: the complement factor *C3* is located in the core network. Also, pattern recognition receptors (PRRs) and other receptors may potentially recognize PrP^{Sc}: *ITGB2* and *TLR2* in the SCC; *CD14*, *CD68*, *FCGR2B*, *TREM2* in the core network. Subsequently, the complement complexes and PRRs may be responsible for stimulating the production of cytokines (*CSF1* in the SCC and *CXCL10* in the core network) and growth factors (*TGFB1* in the SCC). They may also activate astrocytes, indicated by the increased expression of the glial marker *GFAP* in the core network. Cytokines released by microglia and astrocytes then lead to the activation of endothelial cells, which would stimulate the migration of leukocytes from the blood, followed by their differentiation into microglia (leukocyte extravasation), involving *ITGB2*, *NCF1*, *TGFBR1*, *TGFB1* in the SCC and *TGFBR2*, *ITGAX*, *CYBB* in the core. The upregulation of CSF1 (in the SCC) suggests that mononuclear leukocytes (blood monocytes) may be converted into microglia upon entering the brain.

Robustness of the results

In order to assess the effect the stringency in gene selection criteria could have on the network topology and dynamics, we reconstructed two additional networks based on either more relaxed or constraint criteria for the gene selection. This resulted, as expected, in a bigger and smaller network respectively (see Additional file 1).

From the original list of 333 DEGs we selected genes with p-value smaller than 0.01 on at least one time point among three last time points and obtained a list of 226 differentially expressed genes resulting in a network of 27 nodes and 39 edges. Within this network we identified a SCC of 8 nodes and 13 edges (a subset of the original SCC with 16 nodes and 28 edges). This network again showed a key role of genes involved in the inflammatory response and identical dynamical behavior with two stable states matching experimental expression values in healthy and diseased states. The betweenness centrality of this network is significantly different between genes participating in the SCC and genes in the rest of the network. Median betweenness centrality in the SCC and the reduced version of the global networks were 52.8 and 0, respectively; the distributions in the two groups differed significantly (Mann–Whitney Wilcoxon $W = 3$, $n1 = 8$, $n2 = 19$, $p\text{-}value = 2.358\text{e-}5$) supporting the central role of the new regulatory core in the reduced version of the global network.

The fragmentation analysis of this reduced version of the global network produced the following results. The mean of the giant component size for 1000 randomized removals of 16 nodes was 13.88 nodes (standard deviation 3.41), while it was only 5.00 nodes in the case of the removal of the 9 remaining nodes from the original 16 (seven genes from the original 16 belonging to the SCC are not included in this smaller network). The difference between these values is 2.59 times the standard deviation of the random removal values. This indicates that

despite the missing information it is still possible to detect the importance in terms of connectivity of the 9 remaining key genes belonging to the SCC.

Next, we selected additional genes to expand the original network. This time we queried Prion Protein Data Base (www.prion.systemsbiology.net) to include genes previously not regarded as differentially expressed. To limit the size of this extension we applied three step filtering: 1) we looked for genes that could be upstream and downstream of the original network (the same Pathway Studio settings as in constructing original network); 2) p-value less than 0.01 among three last time points of at least one prion-mouse strain combination; 3) sum of p-values from all time points and prion-mouse combinations less than mean. Applying this criteria we obtained a list of 62 additional genes resulting in a network of 119 nodes and 389 edges. Within this network we obtained one SCC of 82 nodes and 320 edges in which the original SCC of 16 genes were embedded. This network showed again a key role of genes involved in the inflammatory response and identical dynamical behavior with two stable states matching experimental expression values in healthy and diseased states. The betweenness centrality is again significantly different between genes participating in the SCC and genes in the rest of the network. Median betweenness centrality in the SCC and the extended version of the global networks were 92.4 and 0, respectively; the distributions in the two groups differed significantly (Mann–Whitney Wilcoxon $W=326$, $n1=83$, $n2=35$, *p-value* = 1.02e-11). However, no significant differences could be found between the betweenness centrality of genes related with immune response and the rest of the genes within the SCC in the expanded network proving lack of topological bias of this group of genes.

The fragmentation analysis of this expanded version of the global network produced the following results. The mean of the giant component size for 1000 randomized removals of 16 nodes was 99.58 nodes (standard deviation 2.76), while it was only 87 nodes in the case of the removal of the 16 genes belonging to the original SCC. The difference between these values is 4.54 times the standard deviation of the random removal values. This indicates that despite the noisy information the 16 nodes belonging to the original SCC still show a remarkable connectivity importance.

In summary, the analysis of these reduced and expanded networks supports the robustness of our findings against both noisy and incomplete information. Despite the lack of detailed mechanistic information about specific pathways we still can gain insights into the importance of neuroinflammation and immune response in prion disease and their impact in the network dynamics and disease progression.

Discussion

Prion diseases are a protein-based infectious diseases of the nervous system that result in progressive and extensive neurodegeneration throughout the brain. The mechanisms leading to neurodegeneration are incompletely understood, but loss of function of $Prion^{C}$, gain-of-toxic function of $Prion^{Sc}$, activation of cellular and in particular ER stress, neuronal death pathways such as autophagy and apoptosis, and chronic brain inflammation all appear to play a role. Experimental *in vitro* or *in vivo* approaches typically investigate one of the potential pathogenic processes at a time, and often quite elegantly demonstrate their relevance in the disease process. However, to investigate which of these processes is the most pathogenic and contributes the most to the disease process, conventional experimental approaches are more

limited. To address this issue, we therefore used a network analysis approach and looked for a set of genes determining the stability of the network using a Boolean dynamical system. By identifying a set of core regulatory genes, most of which are part of the immune response, that can lock a larger gene network into a stable diseased state, we found that it is the process of brain inflammation that is the most likely to play the major pathogenic role in prion disease.

Despite the fact that six of the 333 DEGs described by Hwang *et al.* are related to the oxidative stress response, only one of them is included in our global network (*PRDX6*) and none in the core regulatory network. In neurons, the accumulation of misfolded proteins also leads to endoplasmic reticulum (ER) stress. The normal unfolded protein response (UPR), which is a consequence of the ER stress, should function to clear the misfolded proteins. But it is thought that pro-inflammatory cytokines released by microglia lead to an upregulation of ER stress and an atypical form of UPR in neurons [15-17]. Furthermore, it has been hypothesized that prolonged ER stress activates cell death pathways [17,18]. Cellular stress is one of the possible mechanisms triggering neurodegeneration. Necrosis in acute brain injury is a result of the release of nitric oxide, reactive oxygen species, calcium and glutamate [6]. The role of prion in triggering the stress response is still not understood, but a toxic effect caused by free radicals produced due to an imbalance in the intracellular cupper levels has been previously associated with prion disease and other neurodegenerative diseases [19,20]. Whether this imbalance is due to the loss of function (lack of prion directly or indirectly involved in dismutase activity) or the gain of new functions (aggregation of PrP^{Sc}) is still unclear, but there is evidence that the toxicity results from prion dependent processes (alteration of PrP-mediated signaling, PrP mislocalization and oligomerization) in murine models of scrapie [21].

The Ccaat-enhance binding protein (CEBP) transcription factor family has been implicated in the differentiation of myelomonocytic cells and the regulation of gene expression during the activation of macrophages [22]. The isoform CEBPA regulates the expression of antioxidant proteins. *CEBPA-deficient* mice were found to be susceptible to hyperoxic conditions and prion was one of the DEGs identified, thus suggesting a role of wild type prion in lung injury [23]. Overexpression of the *CEBPD* isoform is observed in Alzheimer's [24] and in prion disease [25]. Colony-stimulating factor 1 (CSF1) and its receptor CSF1R are involved in the process of macrophage DNA synthesis, which is induced by the presence of amyloid beta and prion protein. The presence of misfolded amyloid beta precursor and prion protein promotes macrophage survival in bone marrow cells [26]. Integrin beta 2 is encoded by *ITGB2* and is known to selectively bind to neuronal cells damaged by cleaved prion. It is also involved in neuronal cell killing by activated microglial cells [27]. Transglutaminase 2 is encoded by the *TGM2* gene and may contribute to the cross-linking of soluble peptides preventing amyloid formation of alpha-synuclein or prion protein, thus increasing concentrations of soluble toxic oligomers [28]. Overexpression of *TGM2* is also observed in Huntington and Alzheimer's diseases [29]. *CX3CR1* is part of the complement system and encodes the receptor for the chemokine fractalkine. Antagonists of chemokine receptors have been shown to play a neuroprotective role [30] in several neurodegenerative diseases including prion disease. Also, thiazolopyrimidine derivatives are antagonists of CX3CR1 and have been developed as drugs for prion disease therapy [31]. TGFB1 is a cytokine which is overexpressed in prion disease. Signaling through the TGFB1 receptor is potentially responsible for the chronic inflammatory processes by regulating an atypical microglia phenotype [32]. *LGALS3* encodes galectin-3, a beta-galactoside binding lectin. It has been shown that lectin binding and normal prion (PrP^{C}) glycosylation are altered during aging [33]. STAT1 transcription factor signaling is increased

in mouse models lacking PrP^C, indicating a neuroprotective role of PrP^C [34,35]. The STAT3 transcription factor is important for the anti-apoptotic activity of humanin and therefore for humanin-mediated neuroprotection after Alzheimer disease-related insult [36]. The protective role of humanin was also observed in prion disease [37].

The possible mechanistic links of the remaining genes in the SCC (*TLR2*, *NCF1*, *PTPN6* and *B2M*) to prion disease are still open. Thus, these genes represent a new set with a potential crucial function in prion disease pathogenesis.

The gene product of TLR2, or Toll-like-receptor 2, is a pattern recognition receptor found primarily on innate immunity cells including microglia/macrophages [38,39]). Although toll-like receptors are known to recognize misfolded proteins and trigger stress responses in various neurodegenerative diseases, TLR2 has not been directly linked with the recognition of prion deposition [40]. Interestingly, pharmacological inhibitors of Toll-like-receptors, including TLR2, are being studied for the treatment of various inflammatory diseases [41]). The gene product of NCF1, or Neutrophil-cytosolic-factor 1, is a component of the neutrophil NADPH, and enzyme complex that produces a superoxide anion, a reactive radical[42]. The gene product of PTPN6, also called SHP-1 (Src homology region 2 domain-containing phosphatase-1), codes for Tyrosine-protein-phosphatase non-receptor type 6, a protein tyrosine phosphatase involved in cell differentiation, in particular hematopoetic cells [43]. B2M codes for β_2 microglobulin, a component of MHC class I molecules, and its expression in neurons is regulated during injury [44]. These factors point again to a major involvement of the innate immune system in the pathogenesis of prion disease, and furthermore suggest the existence of new targets for possible therapeutic intervention.

In another transcriptomics study by Sorensen *et al.* [25], C57BL/6 or VM mice were inoculated intracerebrally with three strains of scrapie prion that differed from those used in the study by Hwang *et al.* Seventeen genes were found to be related to inflammation and microglia activation. Ten of these genes were also among the 333 DEG in the study by Hwang *et al.*: six are located in our core network (*ABCA1*, *CLU*, *TF* and *SOX9*) and two in our SCC (*B2M* and *TGFB1*). However, it should be noted that *CLU* was placed in the cell death category and *TF* into the iron homeostasis category by Hwang *et al.* All genes were similarly upregulated in both studies. We decided to follow up with the network analysis of data from the latter publication since it was based on larger number of mice model -prion strain combinations and therefore provided more comprehensive list of DEGs. Although, both Hwang's and Sorensen's studies included analysis aimed on identifying genes related to inflammatory processes, a stability and dynamics analysis of the gene regulatory network was performed for the first time in the present study, allowing for the identification of brain inflammation as the main prion disease process among all the possible others.

Inflammation response could be an overrepresented functional category in a great number of diseases. In the particular case of neurodegenerative diseases belonging to the class of protein misfolding diseases, it is well established that neuroinflammation plays a role. What we consider remarkable and constitutes our main finding is the key role that neuroinflammation plays in the specific case of prion disease, connecting different functional modules and constituting a switch that allows the network to reach a self-maintained disease state, once triggering factors (protein deposition and the formation of amyloid plaques) initiate the process. According to our simulations, the special topology that connects neuroinflammation elements (a cluster of positive feed-back loops or SCC) makes the regulatory core sensitive

under perturbation to easily transit from inactive (healthy) to active (diseased) states but become very stable once the active state is reached.

To experimentally test the role of the genes of the identified master regulatory core in prion disease, we envisage inoculating $Prion^{Sc}$ into knockout mice that are lacking one of the 16 SCC genes. Subsequently, the mice would be analyzed pathologically with regard to neuronal function and death, as well as for DEGs for which the network analysis would be repeated. This analysis would be particularly interesting for the factors whose explicit role has never been demonstrated in prion pathogenesis (*TLR2*, *NCF1*, *PTPN6)*.

Conclusions

In this study, we have carried out a network analysis based on a recent study of prion disease in mouse in order to gain insights into disease progression. We have built a gene regulatory network consisting of genes differentially expressed due to prion disease infection and analyzed network topology and dynamics to identify key network structures in disease progression. We have identified an SCC that plays a crucial regulatory role in the network and is capable of determining network stability. This design resembles the "Medusa model" described by Kauffman [45], in which a set of genes represents a regulatory head and the remaining genes represent arms controlled by the head.

The sixteen genes of SCC we have identified as master regulatory core are capable of activating 58 further genes which are differentially expressed in several mouse prion models. These genes determine the stability of the network and are also the critical connecting element between different pathological processes (disease-causing prion replication and accumulation, immune response and neuronal cell death).

Perturbation analysis of regulatory core genes demonstrates that each gene is individually capable of triggering the transition between two stable states in the larger network. A switch to the "on" state of any of the regulatory core locks the network the new stable, but diseased, state. We hypothesize that this locking may be the cause of the sustained immune response observed in prion disease, which could ultimately lead to prominent neuronal cell death and the manifestation of clinical symptom

Methods

Generation of the global and core regulatory networks

The procedure for the network reconstruction consists of the following steps: a) Obtaining a list of differentially expressed genes. b) Connecting these genes using expression regulatory interactions from literature. c) Determining the core regulatory network.

a) Obtaining a list of differentially expressed genes.

A list of 333 DEGs was extracted from the results of gene expression analysis experiments performed by Hwang *et al.* [4]. These DEGs were found in all five prion-wild type mouse combinations in the study.

b) Connecting differentially expressed genes using gene regulatory interactions described in

literature.

The ResNet mammalian database from Ariadne Genomics http://www.ariadnegenomics.com/) was used to construct a gene regulatory network. The ResNet database includes biological relationships and associations, which have been extracted from the biomedical literature using Ariadne's MedScan technology [46,47]. MedScan processes sentences from PubMed abstracts and produces a set of regularized logical structures representing the meaning of each sentence. The ResNet mammalian database stores information harvested from the entire PubMed, including over 715,000 relations for 106,139 proteins, 1220 small molecules, 2175 cellular processes and 3930 diseases. The focus of this database is solely on human, mouse and rat.

We used the list of differentially expressed genes to build a gene regulatory network without including any additional genes not found in microarray experiments resulting in a raw connected graph of 125 nodes and 255 interactions of known effect (positive or negative).To build the network we included only literature evidences of gene expresion regulation (directed and signed interactions) and is therefore smaller and sparser than it would have been if all possible known interactions had been included (i.e. undirected protein-protein interactions, indirect interactions). The expression patterns of the DEGs were checked in the Prion Database (http://prion.systemsbiology.net) to compare with topology and associations' logic leading to removal of inconsistent 15 nodes and 81 edges. Additionally, discovery of few errors in text mining process lead us to further validation of the network. To avoid false associations we took all sentences used by Pathway Studio (Ariadne Genomics) to determine gene associations and searched for co-occurrence of specific words: modifiers of sentence meaning, indicating increased risk of false interpretation. In the next phase we checked manually highly uncertain sentences and found two clearly wrong associations: CD86 --+>TGFB1 and CEBPA --+>CASP8. In summary, we obtained a final graph of 106 nodes and 169 edges we used for fragmentation analysis in this paper. References for both raw and global network interactions are included in the Additional file 1.

c) Determining the core regulatory network.

Given that only genes with incoming interactions are relevant to the stability analysis, we had to identify genes involved in regulatory feed-back loops, or circuits, and genes regulated by them. For the first task we looked for strongly connected components (SCCs) in the raw network using Binom plugin [48] in Cytoscape [49].

An SCC is a network of nodes, where each node can be accessed directly or indirectly from every other node within the network or, in other words, if there exists a path from each node in the network to every other node. Due to the specific connectivity in a SCC, the information can flow from one node to any other in the structure following at least one path. Such a path has to respect the sense of the interactions (otherwise the component is not strongly but weakly connected). Therefore, the state of any node in the SCC can directly or indirectly affect the state of any other node. This mutual influence between any pair of nodes within the SCC indicates that the SCC may be a relevant stability-related structure. We obtained a single SCC with 16 nodes. After that, we expanded these cores iteratively by adding first neighbors regulated by the SCC until no further neighbors could be added. This yielded a network consisting of the SCC and genes that are directly or indirectly regulated by genes in the SCC (we call this the "core network"). The core network including 74 nodes and 125 interactions (all nodes with incoming interactions) was used for stability and centrality analysis in this

paper. References for the interactions of the core network are included in the Additional file 1.

Stability and perturbation analysis

For the stability analysis we used the SQUAD software package [50], creating a discrete dynamical system that allowed us to identify all the stable states of the system with an asynchronous updating scheme [51] using a binary decision diagram based algorithm [52]. Subsequently, a continuous dynamical system was created to identify the stable states in this continuous model which are located near to the stable states of the discrete system, according to the method described by Mendoza *et al.*, 2006 [53], where the stable states of a Boolean model are taken as initial conditions in the continuous model. Gene perturbations were simulated in the continuous model changing the expression values of specific genes. We also calculated the stability of the SCC in isolation, as well as the stability of the core network. More details about stable states computation and perturbation simulations are included in the Additional file 1.

Network properties

Fragmentation, betweenness centrality and inter-modular participation measurements were employed to compare the properties of SCC genes with other genes in the network, and to determine key genes that might be potential candidates for experimental validation.

In order to test the importance of the SCC in the network's connectivity, we examined the fragmentation effect of removing the 16 nodes belonging to the SCC in comparison with the fragmentation effect of 1000 different randomized removals of 16 nodes in the global network of 106 nodes. The giant component is the biggest connected subgraph found in the network for the given fragmentation and thus a good measure for evaluating such fragmentation [54,55].

Betweenness centrality was computed for all genes in the network. The higher the value, the more central the gene is in the network of reference, i.e. other genes are more likely to be connected along the pathway involving these genes [54] (see Additional file 1).

Modules in the global network were defined by functional and pathological process annotation of genes. The participation coefficient P is a measure quantifying inter-modular connections of genes. For any gene in question P is greater than 0, if odds of inter-modular degree to total degree of the gene is less than 1, which means it has to have at least one connection within its own and neighboring modules. Together with measure of within-module connectivity, participation allows to define role a node in the network ranging from most influential global hub till peripheral node (global hub, connector hub, provincial hub, kinless node, satellite connector, peripheral node and ultra-peripheral node). Such genes connect various functional pathways and might therefore be considered key regulators of cellular processes [56].

Functional analysis

Hwang *et al.* described four pathological features, which were derived from GO attributes: (1) PrP^{Sc} replication and accumulation, (2) microglia/astrocyte activation (which we are calling immune response), (3) synaptic degeneration and (4) neuronal cell death. We mapped

these pathological features on the nodes in our core network and examined how the genes in our network may relate to disease progression.

Authors' contribution

IC participated in network reconstruction and analysis, the design of the study and drafted the manuscript, KR participated in the network reconstruction and analysis, the design of the study and drafted the manuscript, WJ participated in the network reconstruction and analysis, participated in the design and coordination of the study and drafted the manuscript, HK conceived of the study, AdS conceived of the study, participated in its design and coordination and helped to draft the manuscript. All authors read and approved the final manuscript.

Acknowledgements

We thank Dr. Manuel Buttini for helpful discussions and for editing the manuscript. We also thank Dr. Maria Biryukov for helping us with text mining to curate the network.

References

1. Colby DW, Prusiner SB: **Prions.** *Cold Spring Harbor perspectives in biology* 2011, **3**:a006833.

2. Soto C: **Unfolding the role of protein misfolding in neurodegenerative diseases.** *Nat Rev Neurosci* 2003, **4**:49–60.

3. Soto C, Satani N: **The intricate mechanisms of neurodegeneration in prion diseases.** *Trends in molecular medicine* 2010, .

4. Hwang D, Lee IY, Yoo H, Gehlenborg N, Cho JH, *et al*: **A systems approach to prion disease.** *Mol Syst Biol* 2009, **5**:252.

5. Lucin KM, Wyss-Coray T: **Immune activation in brain aging and neurodegeneration: too much or too little?** *Neuron* 2009, **64**:110–122.

6. Amor S, Puentes F, Baker D, van der Valk P: **Inflammation in neurodegenerative diseases.** *Immunology* 2010, **129**:154–169.

7. Hughes MM, Field RH, Perry VH, Murray CL, Cunningham C: **Microglia in the degenerating brain are capable of phagocytosis of beads and of apoptotic cells, but do not efficiently remove PrPSc, even upon LPS stimulation.** *Glia* 2010, **58**:2017–2030.

8. Rezaie P, Lantos PL: **Microglia and the pathogenesis of spongiform encephalopathies.** *Brain Res Brain Res Rev* 2001, **35**:55–72.

9. Wojtera M, Sikorska B, Sobow T, Liberski PP: **Microglial cells in neurodegenerative disorders.** *Folia Neuropathol* 2005, **43**:311–321.

10. Williams A, Lucassen PJ, Ritchie D, Bruce M: **PrP deposition, microglial activation, and neuronal apoptosis in murine scrapie.** *Exp Neurol* 1997, **144**:433–438.

11. Moes M, Le Bechec A, Crespo I, Laurini C, Halavatyi A, *et al*: **A novel network integrating a miRNA-203/SNAI1 feedback loop which regulates epithelial to mesenchymal transition.** *PLoS One* 2012, 7:e35440.

12. Shiraishi T, Matsuyama S, Kitano H: **Large-scale analysis of network bistability for human cancers.** *PLoS Comput Biol* 2010, **6**:e1000851.

13. Sanz J, Cozzo E, Borge-Holthoefer J, Moreno Y: **Topological effects of data incompleteness of gene regulatory networks.** *BMC Syst Biol* 2012, **6**:110.

14. de Silva E, Thorne T, Ingram P, Agrafioti I, Swire J, *et al*: **The effects of incomplete protein interaction data on structural and evolutionary inferences.** *BMC Biol* 2006, **4**:39.

15. Soto C, Satani N: **The intricate mechanisms of neurodegeneration in prion diseases.** *Trends Mol Med* 2010, .

16. Pirot P, Eizirik DL, Cardozo AK: **Interferon-gamma potentiates endoplasmic reticulum stress-induced death by reducing pancreatic beta cell defence mechanisms.** *Diabetologia* 2006, **49**:1229–1236.

17. Malhotra JD, Kaufman RJ: **The endoplasmic reticulum and the unfolded protein response.** *Semin Cell Dev Biol* 2007, **18**:716–731.

18. Kim I, Xu W, Reed JC: **Cell death and endoplasmic reticulum stress: disease relevance and therapeutic opportunities.** *Nat Rev Drug Discov* 2008, 7:1013–1030.

19. Opazo C, Barria MI, Ruiz FH, Inestrosa NC: **Copper reduction by copper binding proteins and its relation to neurodegenerative diseases.** *Biometals: an international journal on the role of metal ions in biology, biochemistry, and medicine* 2003, **16**:91–98.

20. Singh N, Singh A, Das D, Mohan ML: **Redox control of prion and disease pathogenesis.** *Antioxid Redox Signal* 2010, **12**:1271–1294.

21. Aguzzi A, Calella AM: **Prions: protein aggregation and infectious diseases.** *Physiol Rev* 2009, **89**:1105–1152.

22. Tengku-Muhammad TS, Hughes TR, Ranki H, Cryer A, Ramji DP: **Differential regulation of macrophage CCAAT-enhancer binding protein isoforms by lipopolysaccharide and cytokines.** *Cytokine* 2000, **12**:1430–1436.

23. Xu Y, Saegusa C, Schehr A, Grant S, Whitsett JA, *et al*: **C/EBP{alpha} is required for pulmonary cytoprotection during hyperoxia.** *Am J Physiol Lung Cell Mol Physiol* 2009, **297**:L286–298.

24. Li R, Strohmeyer R, Liang Z, Lue LF, Rogers J: **CCAAT/enhancer binding protein delta (C/EBPdelta) expression and elevation in Alzheimer's disease.** *Neurobiol Aging* 2004, **25**:991–999.

25. Sorensen G, Medina S, Parchaliuk D, Phillipson C, Robertson C, *et al*: **Comprehensive transcriptional profiling of prion infection in mouse models reveals networks of responsive genes.** *BMC Genomics* 2008, **9**:114.

26. Hamilton JA, Whitty G, White AR, Jobling MF, Thompson A, *et al*: **Alzheimer's disease amyloid beta and prion protein amyloidogenic peptides promote macrophage survival, DNA synthesis and enhanced proliferative response to CSF-1 (M-CSF).** *Brain Res* 2002, **940**:49–54.

27. Bate C, Boshuizen R, Williams A: **Microglial cells kill prion-damaged neurons *in vitro* by a CD14-dependent process.** *J Neuroimmunol* 2005, **170**:62–70.

28. Konno T, Morii T, Hirata A, Sato S, Oiki S, *et al*: **Covalent blocking of fibril formation and aggregation of intracellular amyloidgenic proteins by transglutaminase-catalyzed intramolecular cross-linking.** *Biochemistry* 2005, **44**:2072–2079.

29. Iismaa SE, Mearns BM, Lorand L, Graham RM: **Transglutaminases and disease: lessons from genetically engineered mouse models and inherited disorders.** *Physiol Rev* 2009, **89**:991–1023.

30. Minami M, Satoh M: **Role of chemokines in ischemic neuronal stress.** *Neuromolecular Med* 2005, 7:149–155.

31. AstraZeneca: *Thiazolopyrimidine derivatives and use thereof as antagonists of the cx3cr1 receptor AstraZeneca AB.*: ; 2007.

32. Cunningham C, Boche D, Perry VH: **Transforming growth factor beta1, the dominant cytokine in murine prion disease: influence on inflammatory cytokine synthesis and alteration of vascular extracellular matrix.** *Neuropathol Appl Neurobiol* 2002, **28**:107–119.

33. Goh AX, Li C, Sy MS, Wong BS: **Altered prion protein glycosylation in the aging mouse brain.** *J Neurochem* 2007, **100**:841–854.

34. Spudich A, Frigg R, Kilic E, Kilic U, Oesch B, *et al*: **Aggravation of ischemic brain injury by prion protein deficiency: role of ERK-1/-2 and STAT-1.** *Neurobiol Dis* 2005, **20**:442–449.

35. Frigg R, Wenzel A, Samardzija M, Oesch B, Wariwoda H, *et al*: **The prion protein is neuroprotective against retinal degeneration *in vivo*.** *Exp Eye Res* 2006, **83**:1350–1358.

36. Hashimoto Y, Suzuki H, Aiso S, Niikura T, Nishimoto I, *et al*: **Involvement of tyrosine kinases and STAT3 in Humanin-mediated neuroprotection.** *Life Sci* 2005, 77:3092–3104.

37. Sponne I, Fifre A, Koziel V, Kriem B, Oster T, *et al*: **Humanin rescues cortical neurons from prion-peptide-induced apoptosis.** *Mol Cell Neurosci* 2004, **25**:95–102.

38. Khoo JJ, Forster S, Mansell A: **Toll-like receptors as interferon-regulated genes and their role in disease.** *Journal of interferon & cytokine research: the official journal of the International Society for Interferon and Cytokine Research* 2011, **31**:13–25.

39. Zeytun A, van Velkinburgh JC, Pardington PE, Cary RR, Gupta G: **Pathogen-specific innate immune response.** *Advances in experimental medicine and biology* 2007, **598**:342–357.

40. Trudler D, Farfara D, Frenkel D: **Toll-like receptors expression and signaling in glia cells in neuro-amyloidogenic diseases: towards future therapeutic application.** *Mediators Inflamm* 2010, .

41. Hennessy EJ, Parker AE, O'Neill LA: **Targeting Toll-like receptors: emerging therapeutics?** *Nature reviews Drug discovery* 2010, **9**:293–307.

42. Babior BM, Lambeth JD, Nauseef W: **The neutrophil NADPH oxidase.** *Arch Biochem Biophys* 2002, **397**:342–344.

43. Chong ZZ, Maiese K: **The Src homology 2 domain tyrosine phosphatases SHP-1 and SHP-2: diversified control of cell growth, inflammation, and injury.** *Histol Histopathol* 2007, **22**:1251–1267.

44. Thams S, Oliveira A, Cullheim S: **MHC class I expression and synaptic plasticity after nerve lesion.** *Brain Res Rev* 2008, **57**:265–269.

45. Kauffman S: **A proposal for using the ensemble approach to understand genetic regulatory networks.** *J Theor Biol* 2004, **230**:581–590.

46. Novichkova S, Egorov S, Daraselia N: **MedScan, a natural language processing engine for MEDLINE abstracts.** *Bioinformatics* 2003, **19**:1699–1706.

47. Daraselia N, Yuryev A, Egorov S, Novichkova S, Nikitin A, *et al*: **Extracting human protein interactions from MEDLINE using a full-sentence parser.** *Bioinformatics* 2004, **20**:604–611.

48. Zinovyev A, Viara E, Calzone L, Barillot E: **BiNoM: a Cytoscape plugin for manipulating and analyzing biological networks.** *Bioinformatics* 2008, **24**:876–877.

49. Smoot ME, Ono K, Ruscheinski J, Wang PL, Ideker T: **Cytoscape 2.8: new features for data integration and network visualization.** *Bioinformatics* 2011, **27**:431–432.

50. Di Cara A, Garg A, De Micheli G, Xenarios I, Mendoza L: **Dynamic simulation of regulatory networks using SQUAD.** *BMC Bioinforma* 2007, **8**:462.

51. Garg A, Di Cara A, Xenarios I, Mendoza L, De Micheli G: **Synchronous versus asynchronous modeling of gene regulatory networks.** *Bioinformatics* 2008, **24**:1917–1925.

52. Garg A, Xenarios I, Mendoza L, DeMicheli G: **An Efficient Method for Dynamic Analysis of Gene Regulatory Networks and in silico Gene Perturbation Experiments Research in Computational Molecular Biology**. In Edited by Speed T, Huang H. Heidelberg: Springer Berlin; 2007:62–76.

53. Mendoza L, Xenarios I: **A method for the generation of standardized qualitative dynamical systems of regulatory networks.** *Theoretical biology & medical modelling* 2006, **3**:13.

54. Newman M, Barabási AL, Watts DJ: *The Structure and Dynamics of Networks.* Princeton, New Jersey: Princeton University Press; 2006.

55. Dobrin R, Beg QK, Barabasi AL, Oltvai ZN: **Aggregation of topological motifs in the Escherichia coli transcriptional regulatory network.** *BMC Bioinforma* 2004, **5**:10.

56. Guimera R, Sales-Pardo M, Amaral LA: **Classes of complex networks defined by role-to-role connectivity profiles.** *Nat Phys* 2007, **3**:63–69.

Additional file

Additional_file_1 as XLS

Additional file 1 Supplementary material

a)

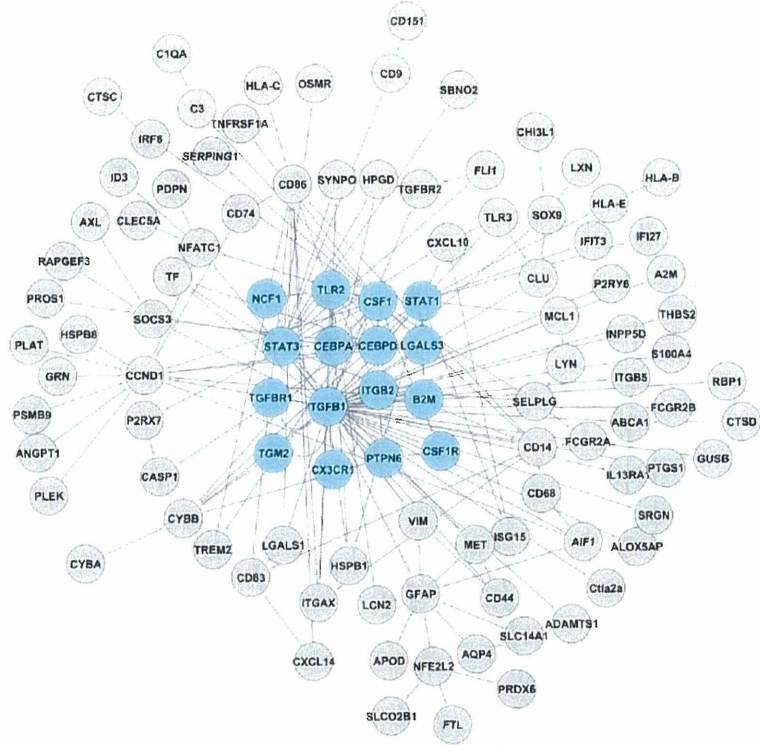
CD151
C1QA
CD9
HLA-C
OSMR
SBNO2
CTSC
C3
TNFRSF1A
CHI3L1
IRF8
SERPING1
ID3
PDPN
CD86
SYNPO
HPGD
TGFBR2
FLI1
LXN
HLA-B
HLA-E
CD74
TLR3
SOX9
AXL
CLEC5A
IFIT3
IFI27
NFATC1
CXCL10
RAPGEF3
TF
CLU
P2RY6
A2M
NCF1
TLR2
CSF1
STAT1
PROS1
SOCS3
MCL1
THBS2
PLAT
HSPB6
STAT3
CEBPA
CEBPD
LGALS3
INPP5D
S100A4
LYN
GRN
CCND1
ITGB5
RBP1
TGFBR1
TGFB1
ITGB2
B2M
SELPLG
FCGR2B
PSMB9
P2RX7
ABCA1
CTSD
CD14
FCGR2A
ANGPT1
TGM2
PTPN6
CSF1R
GUSB
CASP1
CX3CR1
IL13RA1
PTGS1
PLEK
CD68
SRGN
CYBB
VIM
TREM2
LGALS1
MET
ISG15
AIF1
ALOX5AP
CYBA
HSPB1
CD83
Ctla2a
ITGAX
LCN2
GFAP
CD44
ADAMTS1
SLC14A1
CXCL14
APOD
NFE2L2
AQP4
PRDX6
SLCO2B1
FTL

b)

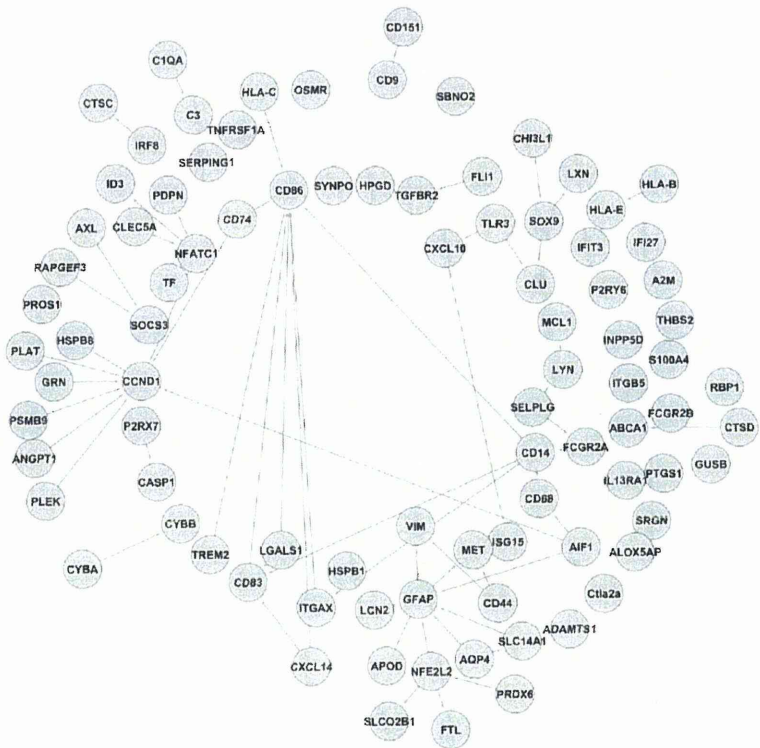
CD151
C1QA
CD9
HLA-C
OSMR
SBNO2
CTSC
C3
TNFRSF1A
CHI3L1
IRF8
SERPING1
ID3
PDPN
CD86
SYNPO
HPGD
TGFBR2
FLI1
LXN
HLA-B
HLA-E
CD74
TLR3
SOX9
AXL
CLEC5A
IFIT3
IFI27
NFATC1
CXCL10
RAPGEF3
TF
CLU
P2RY6
A2M
PROS1
SOCS3
MCL1
THBS2
PLAT
HSPB6
INPP5D
S100A4
LYN
GRN
CCND1
ITGB5
RBP1
SELPLG
PSMB9
P2RX7
FCGR2B
ABCA1
CTSD
CD14
FCGR2A
ANGPT1
GUSB
CASP1
IL13RA1
PTGS1
PLEK
CD68
CYBB
VIM
SRGN
TREM2
LGALS1
MET
ISG15
AIF1
ALOX5AP
CYBA
HSPB1
CD83
Ctla2a
ITGAX
LCN2
GFAP
CD44
ADAMTS1
SLC14A1
CXCL14
APOD
NFE2L2
AQP4
PRDX6
SLCO2B1
FTL

c)

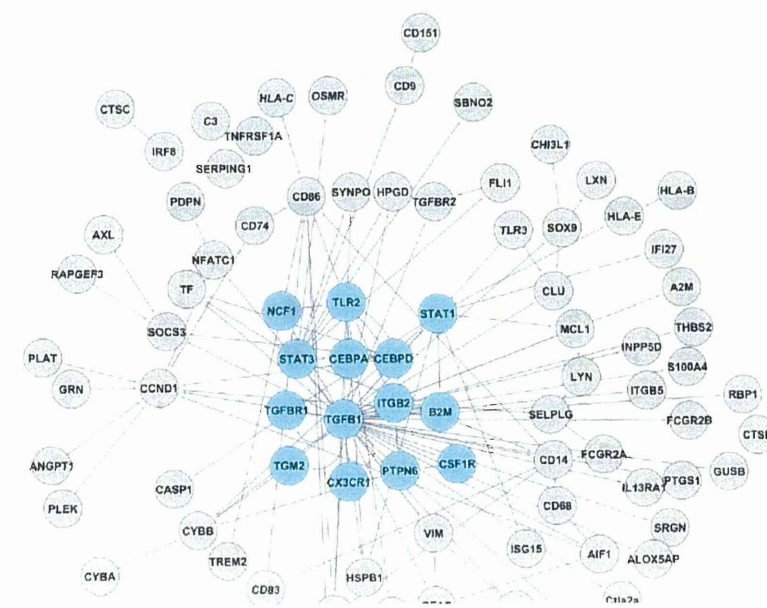
CD151
CD9
HLA-C
OSMR
SBNO2
CTSC
C3
TNFRSF1A
IRF8
CHI3L1
SERPING1
PDPN
CD86
SYNPO
HPGD
TGFBR2
FLI1
LXN
HLA-B
HLA-E
CD74
TLR3
SOX9
AXL
IFI27
NFATC1
RAPGEF3
TF
CLU
A2M
NCF1
TLR2
STAT1
SOCS3
MCL1
THBS2
INPP5D
PLAT
STAT3
CEBPA
CEBPD
S100A4
LYN
GRN
CCND1
ITGB5
RBP1
TGFBR1
TGFB1
ITGB2
B2M
SELPLG
FCGR2B
CTSD
ANGPT1
TGM2
CX3CR1
PTPN6
CSF1R
CD14
FCGR2A
GUSB
CASP1
IL13RA1
PTGS1
PLEK
CD68
CYBB
VIM
SRGN
ISG15
AIF1
TREM2
ALOX5AP
CYBA
HSPB1
CD83
Ctla2a

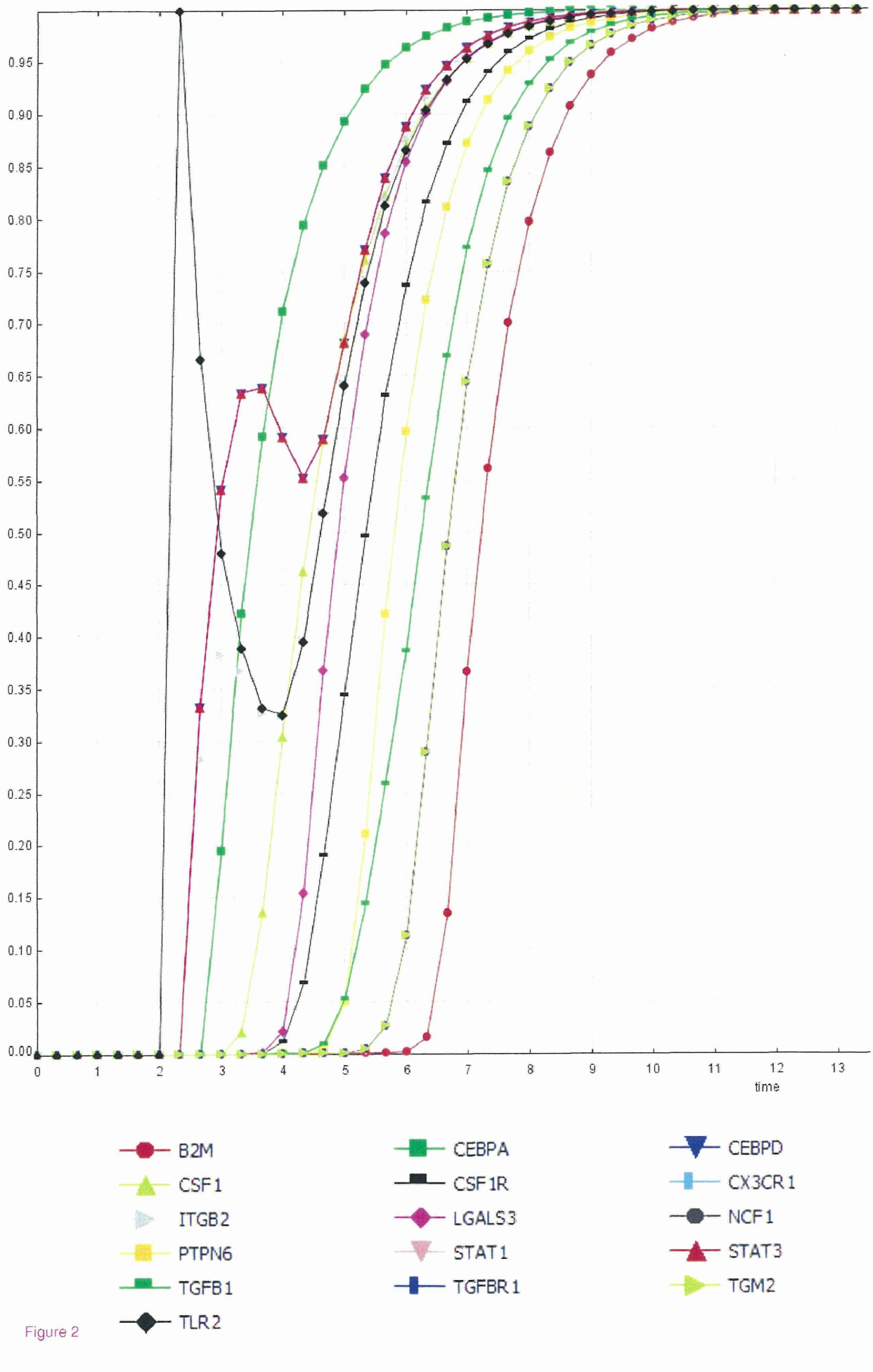
0.95
0.90
0.85
0.80
0.75
0.70
0.65
0.60
0.55
0.50
0.45
0.40
0.35
0.30
0.25
0.20
0.15
0.10
0.05
0.00
0
1
2
3
4
5
6
7
8
9
10
11
12
13
time
B2M
CEBPA
CEBPD
CSF1
CSF1R
CX3CR1
ITGB2
LGALS3
NCF1
PTPN6
STAT1
STAT3
TGFB1
TGFBR1
TGM2
TLR2

Figure 2

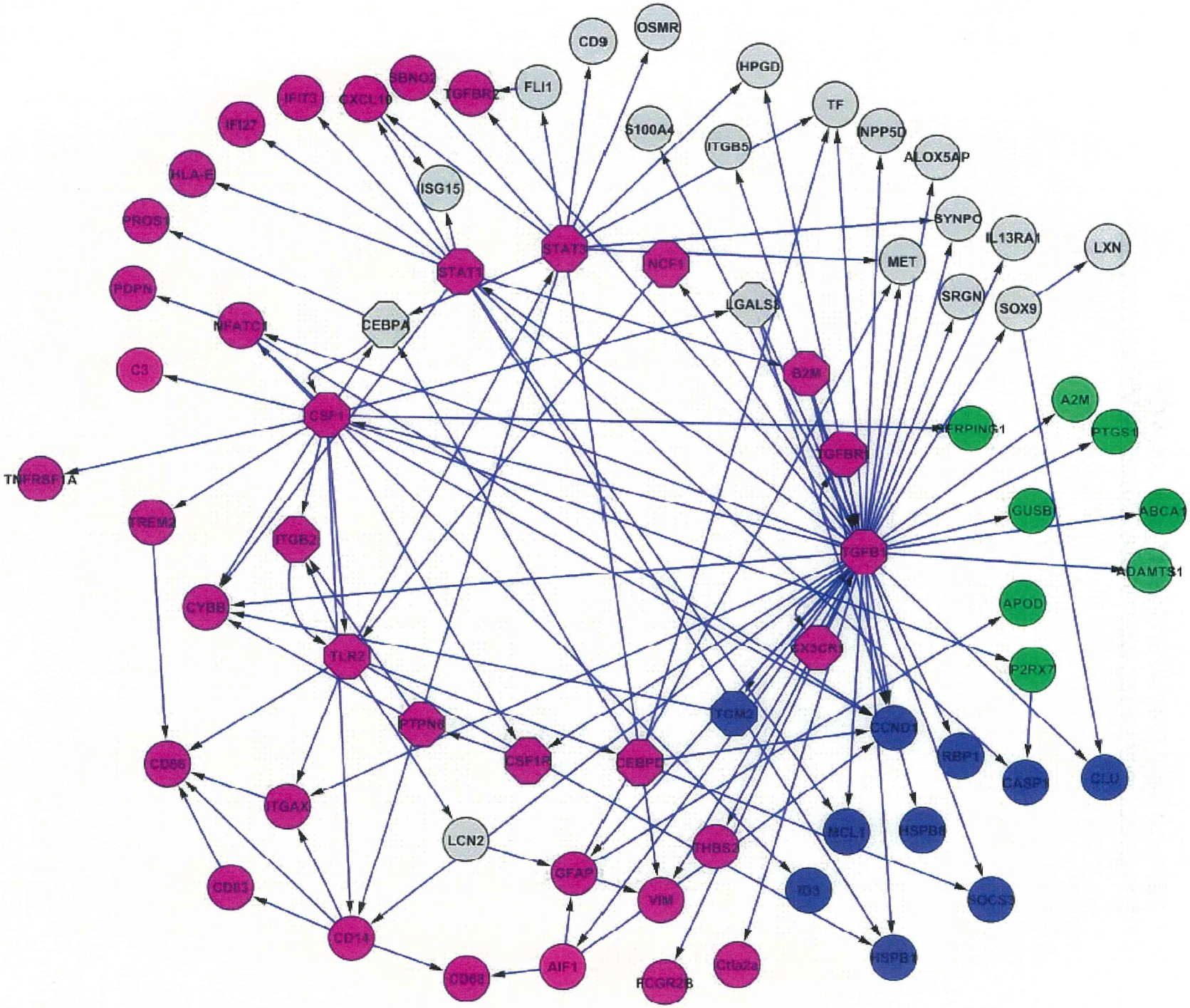
CD9
OSMR
HPGD
FLI1
TF
S100A4
ITGB5
NPP5D
ALOX5AP
ISG15
SYNPO
IL13RA1
LXN
STAT3
STAT1
NCF1
MET
SRGN
SOX9
LGALS3
CEBPA
S2M
A2M
PTGS1
TGFBR1
GUSB
ABCA1
TGFB1
ADAMTS1
APOD
CX3CR1
P2RX7
TGM2
CCND1
RBP1
CASP1
CLU
PTPN6
CSF1R
CEBPB
ITGAX
LCN2
MCL1
HSPB8
THBS2
GFAP
VIM
ID3
SOCS3
CD83
CD14
CD68
AIF1
FCGR2B
Ctla2a
HSPB1

Figure 3

Additional files provided with this submission:

Additional file 1: 9849542347286247_add1.xls, 472K
http://www.biomedcentral.com/imedia/7062869398267316/supp1.xls

Shoemaker et al. BMC Systems Biology 2012, 6:117
http://www.biomedcentral.com/1752-0509/6/117

BMC Systems Biology

RESEARCH ARTICLE Open Access

Integrated network analysis reveals a novel role for the cell cycle in 2009 pandemic influenza virus-induced inflammation in macaque lungs

Jason E Shoemaker[1], Satoshi Fukuyama[1†], Amie J Eisfeld[2†], Yukiko Muramoto[3], Shinji Watanabe[1,2], Tokiko Watanabe[1,2], Yukiko Matsuoka[1,2,4], Hiroaki Kitano[1,4,5,6,7*] and Yoshihiro Kawaoka[1,2,3,8,9*]

Abstract

Background: Annually, influenza A viruses circulate the world causing wide-spread sickness, economic loss, and death. One way to better defend against influenza virus-induced disease may be to develop novel host-based therapies, targeted at mitigating viral pathogenesis through the management of virus-dysregulated host functions. However, mechanisms that govern aberrant host responses to influenza virus infection remain incompletely understood. We previously showed that the pandemic H1N1 virus influenza A/California/04/2009 (H1N1; CA04) has enhanced pathogenicity in the lungs of cynomolgus macaques relative to a seasonal influenza virus isolate (A/Kawasaki/UTK-4/2009 (H1N1; KUTK4)).

Results: Here, we used microarrays to identify host gene sequences that were highly differentially expressed (DE) in CA04-infected macaque lungs, and we employed a novel strategy – combining functional and pathway enrichment analyses, transcription factor binding site enrichment analysis and protein-protein interaction data – to create a CA04 differentially regulated host response network. This network describes enhanced viral RNA sensing, immune cell signaling and cell cycle arrest in CA04-infected lungs, and highlights a novel, putative role for the MYC-associated zinc finger (MAZ) transcription factor in regulating these processes.

Conclusions: Our findings suggest that the enhanced pathology is the result of a prolonged immune response, despite successful virus clearance. Most interesting, we identify a mechanism which normally suppresses immune cell signaling and inflammation is ineffective in the pH1N1 virus infection; a dyregulatory event also associated with arthritis. This dysregulation offers several opportunities for developing strain-independent, immunomodulatory therapies to protect against future pandemics.

Keywords: Influenza, Host response, Microarray, pH1N1, Systems biology

Background

In April of 2009, a new pandemic H1N1 (pH1N1) influenza virus strain emerged in Mexico [1], and the subsequent global pandemic claimed more than 18,000 lives [2]. Human infections with pH1N1 tended to be mild with typical clinical symptoms (e.g., fever, sore throat, vomiting, and occasional diarrhea) [1]. However, in instances where death occurred, autopsies showed necrotizing bronchitis, a symptom that has also been observed in previous pandemics [3,4]. Loss of life during the 2009 pandemic was minor compared to other pandemics (e.g., the 1918 Spanish influenza pandemic, which caused an estimated 50 million deaths worldwide [5]); however, 2009 pH1N1 infections have resulted in more severe illness in young, previously healthy individuals, which is atypical for seasonal influenza virus isolates [6-8].

Currently licensed antiviral compounds against influenza virus (e.g., oseltamavir) interfere with specific functions of viral proteins and are one defense against seasonal and newly emerging pandemic influenza viruses. However,

* Correspondence: kitano@sbi.jp; kawaokay@vetmed.wisc.edu
†Equal contributors
[1]ERATO Infection-Induced Host Responses Project, Saitama 332-0012, Japan
[2]School of Veterinary Medicine, Department of Pathobiological Sciences, Influenza Research Institute, University of Wisconsin-Madison, Madison, WI, USA
Full list of author information is available at the end of the article

the sudden increase in oseltamivir-resistant seasonal H1N1 virus strains in 2007–2008 [9] and the existence of resistant pH1N1 virus isolates [10] strongly underscore the urgent need for the development of novel strategies to alleviate influenza virus-induced disease. As an alternative to directly inhibiting viral proteins, aspects of the host response that strongly correlate with host pathology could be targeted to reduce the overall severity of infection. Such therapies may be more robust against the emergence of drug-resistant strains because they do not target influenza virus-specific gene products, which are subject to drug-mediated selective pressure. Therefore, a better understanding of the mechanisms contributing to influenza virus pathogenesis is needed to provide the basis for the development of novel host-modulatory therapies. We have reported that a pH1N1 isolate (influenza A/California/04/2009 [H1N1], referred to as CA04) is more pathogenic than a seasonal H1N1 isolate in several mammalian models, including cynomolgus macaques [11]. Specifically, CA04-infected macaques exhibited higher body temperatures, more efficient virus replication in both the upper respiratory tract and lungs, increased production of pro-inflammatory cytokines (e.g., CCL2 and IL6), and more severe lung lesions at both early (3 days) and late (7 days) times post-infection. In addition, we observed an increased presence of inflammatory infiltrates in alveolar spaces and more abundant viral antigen staining of both type I and type II pneumocytes. These pathological characteristics are similar to those that distinguish highly pathogenic avian H5N1 and 1918 influenza viruses from lower pathogenicity isolates [12-14], suggesting a common host response theme that may contribute to increased pathogenicity phenotypes for diverse influenza viruses. However, the specific mechanisms underlying the severity of CA04 virus pathogenicity remain to be fully elucidated.

In this study, we undertook a unique bioinformatics approach to identify host processes that might be responsible for the enhanced pathology of CA04 in macaques. Other studies have used microarray analysis in conjunction with bioinformatics tools (e.g., Ingenuity Pathway Analysis (IPA) or DAVID [15]) to dissect the response to influenza virus infection, primarily at the level of the outcome of host signaling (i.e., differentially expressed transcripts) [13,14,16-18]. However, these studies typically have used such tools in isolation, and largely have not attempted to predict causative regulatory influences mediated by factors existing outside of the primary dataset. Here, we have combined process-level and cell-specific functional enrichment analyses of highly differentially expressed transcripts in CA04-infected lung tissues, identification of putative transcription factors involved in regulating differential expression, canonical pathway enrichment, and protein-protein interactions to develop an integrated pathogenicity-associated host response network. This novel approach revealed not only differentially regulated pathways and differences in immune cell populations that correlate with enhanced CA04 pathogenicity, but importantly, also identified critical regulatory intermediaries between these correlates. We suggest that the resulting network can be systematically explored for novel therapeutic intervention.

Results

CA04 may promote inflammation through increased expression of chemotactic molecules and caspase-1 induction and suppression of glutathione S-transferase (GST) expression

The CA04 virus induces more severe lesions in the lungs of cynomolgus macaques relative to a seasonal influenza virus isolate (A/Kawasaki/UTK-4/09 [H1N1; referred to KUTK4]) [11]. To identify host functions and pathway activity that might explain this difference, we compared the global transcriptional response of CA04- and KUTK4-infected lung tissues derived from the animals reported in [11]. Microarray analysis of RNA isolated from within gross lesions identified 101 differentially expressed (DE; See Methods) transcripts between the two infections on day 3 p.i. and 854 DE transcripts on day 7 p.i. More than half of the DE transcripts from day 3 were also DE on day 7, and the overlap between time points was significant (Fisher's Exact test, $P < 10^{-16}$). A table summarizing the DE test results is shown in Additional file 1, and total lists of DE transcripts from days 3 and 7 are available in Additional file 2. It is important to note that, while lung lesion severity varied between samples (Additional file 3), principle component analysis did not identify any relationships between the samples based on lesion severity (data not shown).

We first focused on genes commonly associated with inflammation and apoptosis (Figure 1). Enhanced up-regulation of interferon (IFN)-stimulated genes (ISGs) was observed on day 3 and day 7 p.i., indicating that CA04 induced more robust type I IFN signaling than did KUTK4 (Additional file 1). On day 3 p.i., three chemokines (CCL13, CCL2 and CCL3L3) were more up-regulated with CA04 infection; and these together with four others (CCL11, CCL4, CCL8 and CXCL3) were also more up-regulated on day 7. In general, the up-regulated chemokines perform pleiotropic recruitment activities against multiple immune cell subtypes; however, CCL2 and CCL3L3 exhibit potent chemotactic activity toward monocytes [19,20]. On day 7, we also observed enhanced expression of chemokine receptors that are abundant on monocytes (CCR1 and CCR2), interleukins that are primarily expressed and secreted by macrophages (IL10 and IL1A) and molecules that regulate lymphocyte activities (IL21R, IL4R, and IL7). Collectively, these observations are consistent with detailed histopathology analysis of immune cell infiltrates in macaque lungs infected

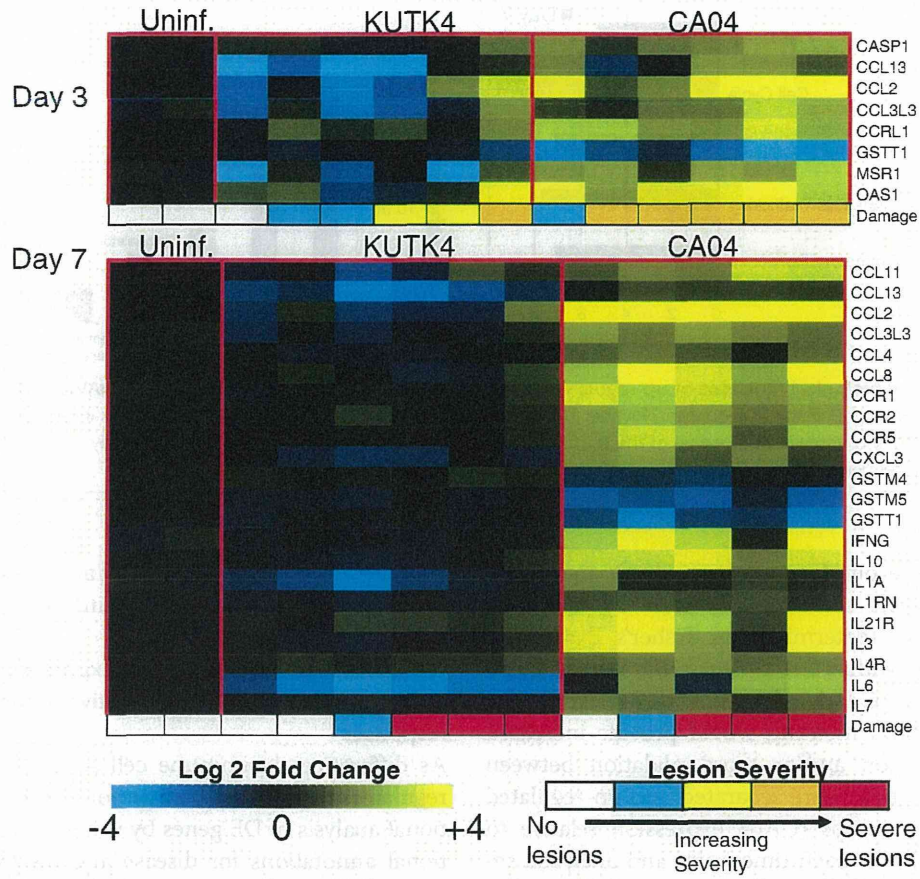

Figure 1 CA04 differentially expressed genes. The transcription profiles of select DE genes on day 3 (top) and day 7 p.i (bottom). Each column represents the gene expression profile of an individual macaque lung tissue sample; gene expression levels for two samples acquired from a uninfected animal are also shown (to the left) for reference. The lesion severity, as described in (11), for each sample is shown at the bottom (Damage) of each heat map. White indicates no lesions; blue represents lung lesions with severe alveolar wall thickening; yellow indicates mild lung lesions with some antigen-positive cells present; orange indicates severe lesions containing a significant number of virus antigen-positive cells; and red indicates severe lung lesions in which the alveolar space was filled with inflammatory cells.

with a similar pH1N1 strain [7], and support the suggested involvement of monocyte and lymphocyte sub-populations in the regulation of CA04 mediated pathology.

Particularly interesting was the observed up-regulation of caspase 1 (CASP1) in CA04-infected lungs. CASP1 is converted to its active form by the inflammasome signaling complex, which is activated by influenza virus infection [21,22]. In turn, CASP1 cleaves latent IL1β and IL18 leading to the secretion of the activated forms of these pro-inflammatory cytokines [23]. Consistent with increased CASP1 expression, IL1β and IL18 protein concentrations were elevated in the lungs of 2 of 3 CA04-infected macaques at day 7 (see Additional files in [11]). Taken together, these observations are indicative of increased inflammasome activity in CA04 infections.

Among the CA04-down-regulated transcripts, we observed several members of the cytosolic glutathione S-transferase (GST) protein family (GSTT1 on day 3; GSTT1, GSTM5, and GSTM4 on day 7). GSTs are antioxidant enzymes that participate in the inactivation of secondary metabolites formed as a result of oxidative stress, and thereby serve a protective role in the cell [24]. Similar suppression of GST transcription was observed in the kidneys of chickens infected with an HPAI virus strain [25], and it has been suggested that oxidative stress may be a key pathway involved in lung injury associated with HPAI virus infection [26]. Thus, the CA04-enhanced down-regulation of GST likely promotes oxidative injury in lung tissue.

CA04-infected macaques exhibit enhanced inflammatory and cell cycle gene expression

IPA and DAVID were next used to identify functional differences between CA04 and KUTK4 infections (Figure 2). IPA uses Fisher's Exact test to determine the enrichment significance for each function annotated in the IPA database. DAVID, on the other hand, uses clusters of related annotations built from several annotation

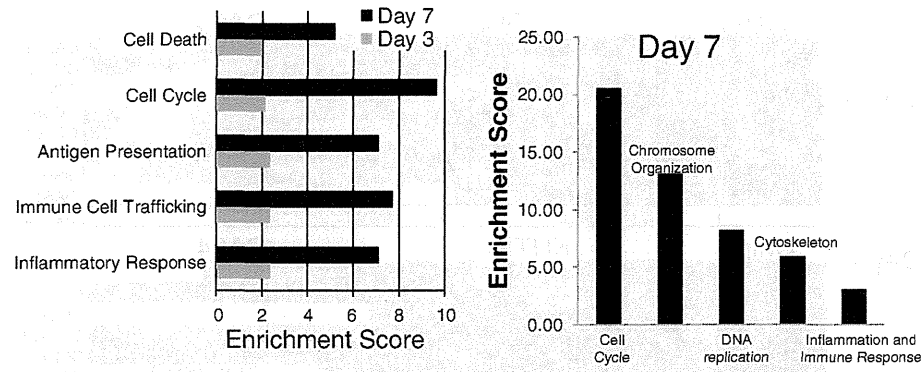

Figure 2 The enriched biological functions of up-regulated genes, as determined by (left) IPA and (right) DAVID. The IPA enrichment score is reported as the -log10 of the FDR-adjusted P-value. DAVID clusters redundant or highly related annotations into clusters and reports the enrichment as the –log10 of the average P-value of the terms in each annotation cluster. DAVID did not identify any significant annotations for genes which were up-regulated on day 3, and only enrichments for day 7 are shown.

databases (e.g., gene ontology, pathway data), and calculates the enrichment score of a cluster by averaging unadjusted *P*-values (determined by Fisher's Exact test) of the annotations within the cluster [15]. We reasoned that analyzing the CA04 pathogenicity-associated DE transcripts using both methods would provide increased functional information and/or cross-validation between methods. DE transcripts were separated into up-regulated or down-regulated groups (CA04 expression relative to KUTK4 expression) for each time point and analyzed separately. All significantly enriched (FDR-adjusted *P*-value < 0.01) IPA functional annotations and DAVID functional clusters are included in Additional files 4 and 5, respectively.

IPA analysis of up-regulated DE transcript identified enrichment for 'Inflammatory Response', 'Immune Cell Trafficking', and 'Antigen Presentation' at day 3 p.i., consistent with the increased immune cell infiltrates observed in the original pathology examination [11]; no significant clusters were identified in this time point using DAVID analysis (Figure 2). Transcripts up-regulated on day 7 were enriched for many of the same IPA categories found on day 3, and both IPA and DAVID identified 'Cell Cycle' as being the most highly enriched, up-regulated process on day 7. More specific categories, such as positive or negative regulation of cell cycle, did not provide conclusive evidence as to the effect of the regulation on cell cycle (see Additional files 5 and 6). Among the downregulated transcripts, we saw enrichment only with IPA at the 7 d p.i. time point, and only in two categories with no obvious connection to the host response to infection (e.g., 'Psychological Disorders' and 'Neurological Diseases') (Additional file 4). These results suggest that functional differences between CA04 and KUTK4 initiate early after infection and are amplified later in the infection, while both analyses identified the cell cycle as the most prominently enriched functional annotation for transcripts that were highly DE with CA04 infection.

CA04 infection enhances gene expression associated with both early/innate and late/adaptive immune cell responses

As differences in immune cell subtypes can also be key regulators of pathology, we performed a cell-specific, functional analysis of DE genes by using IPA's specialized functional annotations for disease and discovery. In addition to providing a general description of function for a category of enriched genes, this approach captures details such as the cell or tissue type in which the gene exerts its function and the orientation of regulation. For down-regulated genes on both days, few categories satisfied our enrichment criteria (FDR-adjusted $P < 0.05$), and no immune cell-specific annotations were enriched. In contrast, the up-regulated gene lists produced more than 500 enriched categories for both days, many of which exhibited functions pertaining to the activation, chemoattraction, infiltration and development of specific immune cell subtypes (a complete list of significant categories for up- and down-regulated genes is shown in Additional file 6). To obtain a clearer representation of how CA04-induced gene expression influences different immune cell subtypes, we categorized enrichment by cell-type and function and employed a heat map to show how the enrichment was distributed in relation to time (summarized in Figure 3; see also Additional files 7 and 8 for a detailed heat map). On day 3, the immune cell subtype most prominently affected by CA04-enhanced gene expression was macrophages, for which categories related to activation, accumulation, and chemotaxis were very highly enriched (Figure 3). T lymphocytes and neutrophils were also broadly affected at this time point, although annotations were not as significant as they were for